Supplemental Material

Glucose 6-phosphate accumulates via phosphoglucose isomerase inhibition in heart muscle

Anja Karlstaedt[1*], M.D., Ph.D., Radhika Khanna[2], B.Sc., Manoj Thangam[3], M.D., and Heinrich Taegtmeyer[1], M.D., D.Phil.

[1] Department of Internal Medicine, Division of Cardiology, McGovern Medical School at The University of Texas Health Science Center at Houston, Houston, TX, USA

[2] Current affiliation: Ross University School of Medicine, Miramar, FL, USA

[3] Current affiliation: Department of Cardiology, Washington University School of Medicine in St. Louis, St. Louis, MO, USA

Address correspondence to:

Anja Karlstaedt, M.D., PhD.

McGovern Medical School at The University of Texas Health Science Center at Houston

6431 Fannin Street, MSB 1.404

Houston, TX, 77030

Email: anja.karlstaedt@uth.tmc.edu

DETAILED METHODS

1. Animals.

All animal experiments were conducted according to the Institutional Animal Care and Use Committee with guidelines issued by The University of Texas Health Science Center at Houston. Animals were fed a standard laboratory chow (LabDiet 5001; PMI Nutrition International, St. Louis, MO, USA). All rats were male Sprague-Dawley rats (10-12 weeks old, 340 to 380 g) obtained from Harlan Laboratories (Indianapolis, IN, USA). Wild type (WT) C57BL/6J mice were obtained from Jackson Laboratory (Bar Harbor, ME, USA), and both male and female mice were used in experiments. Animals were assigned randomly to experimental groups using a Perl 5 (version 5.30.0 for Unix/Linux; www.perl.org) program (see below).

2. Randomizing animals for working heart perfusions.

We randomly assigned wild type Sprague-Dawley rats to experimental groups using a Perl 5 script (version 5.30.0 for Unix/Linux; www.perl.org). Each animal was considered as an element of an array which was randomly shuffled using the shuffle function from the standard List::Util module. This function is a core module of Perl 5 and returns the elements of an array (input list) in a random order. The general algorithm is as follows:

```
use List::Util qw(shuffle);
@array = shuffle(@array);
```

The complete code is provided below:

```
#/usr/bin/perl
use strict;
use warnings;
use List::Util qw(shuffle);
my $replicates = "6";          #experimental replicates
my $totalcages = "9";          #number of animal cages
my $n          = "2";          #number of animals per cages
my @group = map{ ("2mM", "3mM","5mM") } 1..$replicates;
my @cages = map{ 1..$totalcages}c 1..$n;
@group = shuffle(@group);
@cages = shuffle(@cages);
### ouput
print "N\tCage\tGroup\n";
foreach my $i (0..$#cages){
      print $i."\t".$cages[$i]."\t".$group[$i]."\n";
}
```

3. Isolated working rat heart perfusions.

Hearts were perfused by the method described earlier[19]. Briefly, rats (10-12 weeks old, 340 to 380 g) were anesthetized with chloral hydrate (600 mg/kg, intraperitoneal) and heparinized (200 U) through direct injection into the inferior *V. cava* after laparotomy. Next, the chest was opened and the heart rapidly excised and arrested in ice-cold

Krebs-Henseleit (KH) buffer (120 mmol/L NaCl, 5 mmol/L KCl, 1.2 mmol/L $MgSO_4$, 1.2 mmol/L KH_2PO_4, 25 mmol/L $NaHCO_3$, 2.5 mmol/L Ca^{2+}, 5 mmol/L glucose) at pH 7.4. Hearts were mounted on a cannula assembly and perfused in the working heart apparatus at 37°C with KH buffer equilibrated with 95% O_2 – 5% CO_2. The buffer contained glucose as the only exogenous substrate (2, 3, and 5 mmol/L). The filling pressure was 15 cmH_2O with an afterload of 100 cmH_2O from start to min 55 of the perfusion. At this time, epinephrine (1 µmol/L) was added to the buffer, and the afterload was raised to 140 cmH_2O[19, 20]. The cardiac performance was calculated as the product of cardiac output (sum of coronary flow and aortic flow, m^3/min) and the afterload (Pa). Aortic pressure and heart rate were measured continuously with a 3 French catheter (Millar Instruments, Houston, TX, USA) connected to PowerLab 8/30 recording system (ADInstruments, Colorado Springs, CO, USA). At the end of the experiments, the hearts were freeze-clamped with aluminum tongs cooled in liquid N_2 and stored at -80 °C until further use.

4. Determination of glucose oxidation rates with D[U-^{14}C]-glucose.

In working rat heart experiments, hearts were perfused with KH buffer containing D[U-^{14}C]-glucose (20 µCi/L, 9 dpm/nmol), and the coronary effluent was collected every minute. Rates of glucose oxidation were determined by the quantitative collection of $^{14}CO_2$ released in the coronary effluent. Myocardial oxygen consumption (MVO_2) was measured by using YSI 5300A biological monitor (YSI Life Sciences, Yellow Springs, OH, USA). Electrodes were calibrated with air-saturated water (19.6% O_2 saturation after correction for water vapor, 47 mmHg at 37°C). MVO_2 was calculated from the product of the arterial-venous difference and the coronary flow using 1.06 mmol/L for the concentration of dissolved O_2 at 100% saturation.

5. Isolation and culture of AMVMs.

AMVMs were isolated and cultured as described by O'Connell et al.[21]. AMVMs were plated for 1 h in minimal essential media (MEM, cat. no. 11-575-032, Fisher Scientific, Hampton, NH, USA) containing 5.5 mmol/L glucose, 2 mmol/L glutamine, 10% bovine calf serum (HyClone Bovine Calf Serum, 500mL SH30073.03 Fisher Scientific, Hampton, NH, USA), 10 mmol/L butanedione monoxime (BDM, cat. no. B0753-25g, Sigma-Aldrich, St. Louis, MO, USA), and 2 mmol/L ATP (cat. no. A6419-5g, Sigma-Aldrich, St. Louis, MO, USA). AMVMs were maintained in MEM culture media containing 5.5 mmol/L glucose, 2 mmol/L glutamine, 0.1% bovine serum albumin, 10 mmol/L BDM, 200 U Penicillin (cat. no. P7794-10MU, Sigma-Aldrich, St. Louis, MO, USA), and 6.3 U insulin (prepared from an insulin-transferring sodium selenite media supplement; cat. no. I1884-1VL, Sigma-Aldrich, St. Louis, MO, USA). AMVMs were cultured on tissue culture plates coated with 10 µg/mL laminin (CB-40232 Fisher

Scientific, Hampton, NH, USA) in a 2% CO_2 environment at 37 °C.

6. Measurement of intracellular metabolites.

Equal amounts of frozen heart tissue were deproteinized in ice-cold perchloric acid (6%) and homogenized with a 1 mL Dounce homogenizer. The suspension was immediately centrifuged (3,000 g for 10 min at 4°C). The supernatant fraction was transferred into a new microtube and neutralized with buffered KOH. Adenine nucleotides (ATP, ADP, AMP) and G6P were measured in extracts and adjusted to pH 5 with KOH. Metabolite concentrations were assessed colorimetrically using established enzymatic assays, as described previously by Goodwin et al [1].

7. Measurement of enzymatic activity.

Hexokinase. Samples of extracted proteins (20 µg) were added to the HK assay buffer (40 mmol/L triethanolamine buffer at pH 7.6, 222 mmol/L glucose, 8 mmol/L $MgCl_2$, 0.91 mmol/L $NADP^+$, 0.64 mmol/L ATP, 0.55 U/mL GAPDH). The reaction was initiated immediately after mixing all the reagents and the sample. The reduction of $NADP^+$ to NADPH was followed at 37°C by measuring the optical density (OD) at 340 nm.

Lactate dehydrogenase. Samples of extracted proteins (20 µg) were added to the lactate dehydrogenase (LDH) assay buffer (94.5 mmol/L phosphate buffer at pH 7.0, 0.77 mmol/L pyruvate, 0.2 mmol/L NADH). The reaction was initiated immediately after mixing all the reagents and the sample. The oxidation of NADH to NAD^+ was followed at 37°C by measuring the OD at 340 nm.

Malate dehydrogenase. Samples of extracted proteins (20 µg) were added to the malate dehydrogenase (MDH) assay buffer (0.1 mol/L phosphate buffer at pH 7.5, 2 mg/mL oxaloacetic acid, 10 mg/mL NADH). The reaction was initiated immediately after mixing all the reagents and the sample. The oxidation of NADH to NAD^+ was followed at 37°C by measuring the OD at 340 nm.

Glutamate dehydrogenase. Samples of extracted proteins (20 µg) were added to the glutamate dehydrogenase (GLDH) assay buffer (50 mmol/L triethanolamine buffer with 3.6 mmol/L EDTA at pH 8.0, 7 mmol/L oxaloacetic acid, 100 mmol/L ammonium acetate, 0.2 mmol/L NADH, 1 mmol/L ADP, 2 U/mL LDH). The reaction was initiated immediately after mixing all the reagents and the sample. The oxidation of NADH to NAD^+ was followed at 37°C by measuring the OD at 340 nm.

Phosphofructokinase. Samples of extracted proteins (20 µg) were added to the phosphofructokinase (PFK) buffer/substrate solution (70 mmol/L Tris buffer, 1.4 mmol/L $MgSO_4$, 0.71 mmol/L phosphoenolpyruvate, 0.64 mmol/L fructose-1,6-phosphate, 1.8 mmol/L fructose 6-phosphate, 1.1 mmol/L ATP, 0.4 mmol/L NADH, 4.2 U/mL pyruvate kinase, 9.6 U/mL LDH). The reaction was initiated immediately after mixing all the

reagents and the sample. The oxidation of NADH to NAD^+ was followed at 37°C by measuring the OD at 340 nm.

Glucose 6-phosphate dehydrogenase. Samples of extracted proteins (20 µg) were added to the glucose-6-phosphate dehydrogenase (G6PDH) assay buffer (50 mmol/L triethanolamine buffer at pH 7.5, 0.67 mmol/L G6P, 0.5 mmol/L $NADP^+$). The reaction was initiated immediately after mixing all the reagents and the sample. The reduction of $NADP^+$ to NADPH was followed at 37 °C by measuring the OD at 340 nm.

Phosphoglucose isomerase. Samples of extracted proteins (50 µg) were added to the PGI buffer/substrate solution (0.1 mol/L borate buffer at pH 7.8, 7 mmol/L G6P) and incubated for 30 min at 37°C. To one volume buffer/substrate solution, nine-volume color reagents (9 mmol/L resorcinol, 33 mmol/L thiourea) were added and heated for 15 min at 75°C. The OD at 405 nm was measured and compared to a blank reading. Readings were compared to a 0.3 mmol/L fructose standard solution.

Pyruvate kinase. Samples of extracted proteins (20 µg) were added to the pyruvate kinase (PK) buffer/substrate solution (30 mmol/L $MgSO_4$, 10 mmol/L ADP, 36 U/mL LDH, 5 mmol/L phosphoenolpyruvate (PEP), 0.25 mmol/L NADH). The reaction was initiated immediately after mixing all the reagents and the sample. The oxidation of NADH to NAD^+ was followed at 37°C by measuring the OD at 340 nm.

8. Western blotting and immunoprecipitation.

Tissue homogenates for western blotting were prepared in the presence of phosphatase (Sigma-Aldrich, St. Louis, MO, USA) and protease (Roche Applied Science, Penzberg, Germany) inhibitors. Proteins were separated on 4-20% SDS-PAGE gels, transferred to PVDF membranes and probed with antibodies from Cell Signaling Technology (CS, Danvers, MA, USA) against mTOR (CS, cat. no. 2972S), Phospho-mTOR (CS, cat. no. 2971S), AMPK (CS, cat. no. 5832S), Phospho-AMPK (CS, cat. no. 2335S), HKII (CS, cat. no. 6521), TSC2 (CS, cat. no. 3612S), Phospho-Tuberin/TSC2 (Ser1387) (CS, cat. no. 5584S) and GAPDH (CS, cat. no. 5174S), p70 S6 kinase (CS, cat. no. 9202S), Phospho-p70 S6 kinase (Thr421/Ser424) (CS, cat. no. 9204), and PGI (cat no. H00002821-D01, Abnova, Taipei City, Taiwan). Protein levels were detected by immunoblotting using horseradish peroxidase-conjugated secondary antibodies and chemiluminescence. For immunoprecipitation experiments, cultured adult mouse ventricular cardiomyocytes (AMVMs) were washed with ice-cold PBS twice and lysed in hypotonic/digitonin buffer (20 mmol/L PIPES [pH 7.2], 5 mmol/L EDTA, 3 mmol/L $MgCl_2$, 10 mmol/L glycerophosphate, 10 mmol/L pyrophosphate, 0.02% digitonin) containing protease and phosphatase inhibitors. Heart tissue samples were homogenized in the same hypotonic/digitonin buffer using Dounce homogenizers. After 40 min nutation at 4ºC, samples were centrifuged at 20,000 x g for 7 min and the supernatant was transferred into new microcentrifuge tubes. mTOR was immunoprecipitated using

antibody against mTOR (CS, cat. no. 2972S). Cell and tissue lysates were incubated (150 to 300 µg of total protein) with mTOR antibody (4 µg) at 4ºC overnight. Immunocomplexes were then incubated with protein A/G PLUS-agarose beads for 2 h (Pierce, 30 µL of 50 % slurry). Samples were washed with ice-cold lysis buffer four times, and beads were incubated in 2x LDS buffer (~30 µL) for 15 min at 37ºC to elute captured protein and subjected to Western blotting. Signals were quantified by densitometry using NIH ImageJ software (Bethesda, MA, USA). Target protein bands were normalized to that of loading controls obtained from the same blot (e.g., GAPDH for whole cell lysate and target molecule of immunoprecipitation for the study of HKII and mTOR interaction), and normalization factors were calculated for each blot.

9. Measurement of newly synthesized proteins using Click-IT chemistry.

Measurement of newly synthesized proteins was conducted using L-Azidohomoalanine (AHA), as described by Ma et al.[2]. Adult mouse ventricular cardiomyocytes (AMVMs) were cultured with vehicle (phosphate buffered saline, PBS; control) or erythrose 4-phosphate (E4P, 3 µM) in the presence of 2-deoxyglucose (2DG, 25 mmol/L) or cycloheximide (CHX; 10 µg/ mL). AMVMs were cultured for one hour with minimal essential media (MEM) without methionine and pulsed for two hours with MEM culture medium containing AHA (50 µg/mL). AMVMs were harvested, lysed and resuspended in 200 µL of lysis buffer (Dulbecco's phosphate-buffered saline, DPBS; cat. no. 14190-136, Gibco, Thermo Fisher Scientific, Hampton, NH, USA) containing protease (Roche Applied Science, Penzberg, Germany, cat. no. 04693124001) inhibitors, and sonicated for 10 s on ice, followed by 1 min incubation on ice. The sonication was repeated twice. Protein concentration was determined using a Pierce BCA Protein Assay Kit (cat. no. 23225, Thermo Fisher Scientific, Hampton, NH, USA). Samples were centrifuged (21,000 g for 10 min at 4°C). The supernatant fraction was separated into five aliquots, and the pellets were resuspended in 100 µL of 0.5% (wt/vol) SDS (cat. no. 15553-035, Invitrogen, Thermo Fisher Scientific, Hampton, NH, USA) in DPBS. The suspensions were sonicated and boiled for 10 min at 100 °C. After cooling to room temperature, pellet suspensions were divided into five aliquots. The click reaction mixture was prepared fresh using the following reagents: 1 mmol/L copper sulfate (cat. no. 451657, Sigma-Aldrich, St. Louis, MO, USA), 100 µM biotin-PEG4-alkyne (cat. no. TA105-25, Click Chemistry Tools, Scottsdale, AZ, USA), 100 µM Tris[(1-benzyl-1H-1,2,3-triazol-4-yl)methyl]amine (TBTA; cat. no. 678937, Sigma Aldrich, St. Louis, MO, USA), 1 mmol/L Tris(2-carboxyehtyl)phosphine hydrochloride (TCEP, cat. no. C4706-2g, Sigma-Aldrich, St. Louis, MO, USA). To each aliquot (pellet and supernatant fraction), 54 µL of the click reaction mixture was added, and DPBS was used to bring the reaction volume to 400 µL. Each sample was vortexed and incubated for one h at room temperature. All aliquots were combined from the same sample, and trichloroacetic acid (TCA; cat. no.

T0699, Sigma-Aldrich, St. Louis, MO, USA) was added in a 1:4 (vol/vol) ratio to precipitate proteins at 4°C on a rotator overnight. After overnight incubation, samples were centrifuged (3,000 g for 30 min at 4°C). The pellets were resuspended and washed using ice-cold acetone three times. After the last acetone wash, samples were centrifuged (17,000 g for 10 min at 4°C). Based on the initial protein concentration samples were resuspended in LDS buffer. Western blotting was conducted to provide a relative measurement of newly synthesized proteins using HRP-conjugated streptavidin antibody (cat. no. MA1-20010, Thermo Fisher Scientific, cat. no. MA1-20010, Hampton, NH, USA).

10. Metabolic control analysis (MCA).

The analysis was based on *CardioGlyco* (see below for details). The flux control in glycolysis was evaluated, and the influence of enzyme inhibition on the flux control was investigated. The flux control coefficients (FCCs) are defined as follows:

$$C_{v_k}^{J_j} = \frac{v_k}{J_j}\frac{\delta J_j}{\delta v_k} \quad (1)$$

where δv_k denotes the change in the activity of a reaction k, while all other parameters and concentrations are kept constant, and J_j specifies the steady state flux through the j th branch of a pathway. The elasticity coefficient ε quantifies the change of a reaction rate v_i in response to a change in concentration S_j, while everything else is kept fixed.

$$\varepsilon_{S_j}^{i} = \frac{S_j}{v_i}\frac{dv_i}{dS_j} \quad (2)$$

S_j is the concentration of the jth metabolite, and v_i is the rate of the i th reaction. The sum over all products of the FCCs with respect to step i and the elasticity coefficients of the same step is zero:

$$\sum_{i=1}^{L} C_i^{J_j}\, \varepsilon_{S_k}^{i} = 0 \quad (3)$$

$$j \in \{1, \dots, L\}$$

$$k \in \{1, \dots, K\}$$

Calculations of control and ε-elasticity coefficients were conducted using COPASI [3]. Elasticity coefficients were normalized (scaled) to the metabolite concentrations and fluxes in the reference steady-state using the in-build COPASI function.

11. Flux balance analysis. Simulations were conducted using the mathematical model of mammalian cardiac metabolism – *CardioNet*[4]. Simulations were run with boundary

conditions reflecting the metabolite composition of the perfusion buffer and experimentally measured uptake and release rates for glucose (v_{glc}), lactate (v_{lac}), and oxygen ($vMVO_2$). We included measured glucose oxidation rates from *ex vivo* tracer studies into the FBA. At the same time, various metabolites, including amino acids and lipids, were set to previously reported values[4] to determine whether they contribute to ATP production and anaplerosis of Krebs cycle intermediates. The following flux balance analysis was applied to identify steady-state flux distributions that agree with applied substrate uptake and release rates:

$$max v_{ATPase} \tag{4}$$

s.t.

$$S \cdot v = 0 \tag{5}$$

$$v_i^{(-)} \leq v_i \leq v_i^{(+)} \tag{6}$$

$$L_j^{(-)} \leq v_j \leq L_j^{(+)} (j = j_1, j_2, \dots) \tag{7}$$

where v_j denotes the measured glucose oxidation rate, metabolite uptake, or secretion rate through reaction j.

12. Computational Model - *CardioGlyco*

Kinetic rate equations for enzymes used in the model have been modified from previously reported equations.

Glucose Transport (GLUT)

Glc(ext) <=> Glc(int)

$$v_{(GLUT)} = \frac{\frac{Vmax_1 * (Glc_{ext} - Glc_i)}{Kglc_1}}{1 + \frac{(Glc_{ext} + Glc_i)}{Kglc_1} + \frac{Ki_1 * Glc_{ext} * Glc_i}{Kglc_1^2}}$$

(Eq. 1)

Parameters Online Table I

Hexokinase (HK) EC 2.7.1.1

Glc(int) + ATP <=> G6P + ADP

$$v_{HK} = \frac{Vmax_2 * (\frac{Glc_i * ATP}{Kglc_2 * Katp_2} - \frac{G6P * ADP}{Kglc_2 * Katp_2 * Keq_2})}{(1 + \frac{Glc_i}{Kglc_2} + \frac{G6P}{Kg6p_2}) * (1 + \frac{ATP}{Katp_2} + \frac{ADP}{Kadp_2})}$$

(Eq. 2)

Parameters Online Table II

Phosphoglucose isomerase (PGI) EC 5.3.1.9

G6P <=> F6P

$$v_{PGI} = \frac{Vmax_3 * (\frac{G6P}{Kg6p_3} - \frac{F6P}{Kg6p_3 * Keq_3})}{(1 + \frac{G6P}{Kg6p_3} + \frac{F6P}{Kf6p_3})}$$

(Eq. 3)

Parameters Online Table III

Phosphofructosekinase (PFK) EC 2.7.1.11

The rate equation for PFK was based on Hulme E.C. et al. from ox heart PFK [5, 6], and work by Pogson, C.I. et al. [7]

ATP + F6P → ADP + F1,6-P_2

$$v_{PFK} = \frac{Vmax_4 * gR_4 * \frac{F6P}{Kf6p_4} * \frac{ATP}{Katp_4} * (1 + \frac{F6P}{Kf6p_4} + \frac{ATP}{Katp_4} + \frac{\frac{gR_4 * F6P}{Kf6p_4} * ATP}{Katp_4})}{(1 + \frac{F6P}{Kf6p_4} + \frac{ATP}{Katp_4} + \frac{\frac{gR_4 * F6P}{Kf6p_4} * ATP}{Katp_4})^2 + L0_4 * (\frac{1 + \frac{Ciatp_4 * ATP}{Kiatp_4}}{1 + \frac{ATP}{Kiatp_4}})^2 * (\frac{1 + \frac{Camp_4 * AMP}{Kamp_4}}{1 + \frac{AMP}{Kamp_4}})^2 * (1 + \frac{Catp_4 * ATP}{Katp_4})^2 (\frac{1 + \frac{Cf26_4 * F26P2}{Kf26_4} + \frac{Cf16_4 * F16P2}{Kf16_4}}{1 + \frac{F26P2}{Kf16_4} + \frac{F16P2}{Kf16_4}})^2}$$

(Eq. 4)

Parameters Online Table IV

Aldolase (ALD) EC 4.1.2.13

F1,6-P2 <=> DHAP + G3P

$$v_{Ald} = \frac{Vmax_5 * (\frac{F16bP}{Kf16bp_5} - \frac{DHAP * GAP}{Kf16bp_5 * Keq_5})}{(1 + \frac{F16bP}{Kf16bp_5} + \frac{DHAP}{Kdhap_5} + \frac{GAP}{Kgap_5} + \frac{F16bP * GAP}{Kf16bp_5 * Kigap_5} + \frac{DHAP * GAP}{Kdhap_5 * Kgap_5})}$$

(Eq. 5)

Parameters Online Table V

Triosephosphate isomerase (TPI) EC 5.3.1.1

DHAP <=> G3P

$$v_{TPI} = (Kdhap_6 * DHAP - Kg3p * G3P)$$

(Eq. 6)

Parameters Online Table VI

3-Phosphoglycerate kinase (PGK) EC 2.7.5.3

ADP + BPG <=> ATP + P3G

$$v_{PGK} = \frac{Vmax_7 * (\frac{Keq_8 * BPG * ADP - P3G * ATP}{Kp3g_7 * Katp_7})}{(1 + \frac{BPG}{Kbpg_7} + \frac{P3G}{Kp3g_7}) * (1 + \frac{ADP}{Kadp_7} + \frac{ATP}{Katp_7})}$$

(Eq. 7)

Parameters Online Table VII

Phosphoglyceromutase (PGM) EC 4.2.1.11

P3G <=> P2G

$$v_{PGM} = \frac{Vmax_8 * (\frac{P3G}{Kp3g_8} - \frac{P2G}{Kp3g_8 * Keq_8})}{1 + \frac{P3G}{Kp3g_8} + \frac{P2G}{Kp2g_8}}$$

(Eq. 8)

Parameters Online Table VIII

Enolase (ENO)

P2G <=> PEP

$$v_{Eno} = \frac{Vmax_9 * (\frac{P2G}{Kp2g_9} - \frac{PEP}{Kp2g_9 * Keq_9})}{1 + \frac{P2G}{Kp2g_9} + \frac{PEP}{Kpep_9}}$$

(Eq. 9)

Parameters Online Table IX

Pyruvate kinase (PK) EC 2.7.1.40

ADP + PEP <=> ATP + Pyr

$$v_{PK} = \frac{Vmax_{11} * (\frac{PEP * ADP}{Kpep_{10} * Kadp_{10}} - \frac{PYR * ATP}{Kpep_{10} * Kadp_{10} * Keq_{10}})}{(1 + \frac{PEP}{Kpep_{10}} + \frac{PYR}{Kpyr_{10}}) * (1 + \frac{ADP}{Kadp_{10}} + \frac{ATP}{Katp_{10}})}$$

(Eq. 10)

Parameters Online Table X

Pyruvate decarboxylase (PDC) EC 4.1.1.1

Pyr → CO2

$$v_{PDC} = \frac{Vmax_{12} * (\frac{PYR}{Kpyr_{12}})^{nH11}}{1 + (\frac{PYR}{Kpyr_{11}})^{nH11}}$$

(Eq. 11)

Parameters Online Table XI

Adenylate kinase (AK) EC 2.7.4.3

AMP + ATP <=> 2 * ADP

$$v_{AK} = K_{12} * (AMP + ATP) - K_{13} * (ADP)$$

(Eq. 12)

Parameters Online Table XII

Glycerol-3-phosphate dehydrogenase (GPDH) EC 1.1.1.8

DHAP + NADH → NAD + glycerol

$$v_{G3PD} = \frac{Vmax_{14}{}^{*}(\frac{DHAP}{Kdhap_{14}}{}^{*}\frac{NADH}{Knadh_{14}} - \frac{Glycerol}{Kdhap_{14}}{}^{*}\frac{NAD}{Knadh_{14}}{}^{*}\frac{1}{Keq_{14}})}{(1+\frac{DHAP}{Kdhap_{14}}+\frac{Glycerol}{Kglycerol_{14}})^{*}(1+\frac{NADH}{Knadh_{14}}+\frac{NAD}{Knad_{14}})}$$

(Eq. 13)

Parameters Online Table XIII

Lactate transport (LacT)

Lac(ext) <=> Lac

$$v_{LacT} = Vmax_{15}{}^{*}(Lac_{ext} - \frac{Lac}{Keq_{15}})$$

(Eq. 14)

Parameters Online Table XIV

Lactate dehydrogenase (LDH) EC 1.1.1.27

NADH + Pyr <=> Lac + NAD

$$v_{LDH} = Vmax_{16}{}^{*}(Pyr^{*}NADH - \frac{Lac^{*}NAD}{Keq_{16}})$$

(Eq. 15)

Parameters Online Table XV

Glyceraldehyde-3-phosphate dehydrogenase (GAPDH) EC 1.2.1.12

G3P + NAD <=> NADH + BPG

$$v_{GAPDH} = \frac{\frac{Vmax_{17}}{(Knadh_{17}{}^{*}Kg3p_{17})}{}^{*}(NAD^{*}G3P - \frac{BGP^{*}NADH}{Keq_{17}})}{(1+\frac{NAD}{Knad_{17}})^{*}(1+\frac{G3P}{Kg3p_{17}}) + (1+\frac{NADH}{Knadh_{17}})^{*}(1+\frac{BGP}{Kbgp_{17}}) - 1}$$

(Eq. 16)

Parameters Online Table XVI

Glycogen synthesis (GS)

Glycogen plays an important role in cardiomyocytes as an endogenous source for glucose. A simplified rate equation for glycogen synthesis was included based on Kashiwaya et al. [8].

$$\text{ATP + G6P} \rightarrow \text{ADP + glycogen}$$

$$v_{GS} = Katp_{18}{}^{*}(ATP + G6P) \qquad \textit{(Eq. 17)}$$

Parameters Online Table XVII

ATP consumption (ATPase)

Cardiomyocytes have a high rate of ATP provision and turnover to maintain cardiac work. A cardiac ATP consumption rate is included in this model based on beating canine heart experiments [9].

$$\text{ATP} \rightarrow \text{ADP} + \text{P}_\text{i} + \text{H}^+$$

$$v_{ATPase} = Katp_{19}{}^{*}ATP \qquad \textit{(Eq. 18)}$$

Parameters Online Table XVIII

13. *Expansion of CardioGlyco - Pentose phosphate pathway*

Glucose 6-phosphate dehydrogenase (G6PDH)

$$\text{G6P + NADP+} \rightarrow \text{P6GL + NADPH}$$

$$v_{G6PDH} = \frac{Vmax_{18}{}^{*}(\frac{G6P}{Kg6p_{18}}{}^{*}\frac{NADP}{Knadp_{18}} - \frac{6PGL}{K6pgl_{18}}{}^{*}\frac{NADPH}{Knadph_{18}})}{(1 + \frac{G6P}{Kg6p_{18}} + \frac{6PGL}{K6pgl_{18}})^{*}(1 + \frac{NADP}{Knadp_{18}} + \frac{NADPH}{Knadph_{18}})} \qquad \textit{(Eq. 19)}$$

Parameters Online Table XXII

Gluconolactonase (GL)

$$\text{P6GL} \rightarrow \text{P6G}$$

$$v_{GL} = \frac{Vmax_{19}{}^{*}(\frac{6PGL}{K6pgl_{19}}{}^{*}\frac{6PG}{K6pg_{19}})}{(1 + \frac{6PGL}{K6pgl_{19}} + \frac{6PG}{K6pg_{19}})} \qquad \textit{(Eq. 20)}$$

Parameters Online Table XXIII

6-Phosphogluconate dehydrogenase (6PGDH)

P6G + NADP → R5P + NADPH

$$v_{6PGDH} = \frac{Vmax_{20}*(\frac{P6G}{Kp6g_{20}}*\frac{NADP}{Knadp_{20}} - \frac{R5P}{Kr5p_{20}}*\frac{NADPH}{Knadph_{20}})}{\left(1+\frac{P6G}{Kp6g_{20}}+\frac{R5P}{Kr5p_{20}}\right)*(1+\frac{NADP}{Knadp_{20}}+\frac{NADPH}{Knadph_{20}})}$$

(Eq. 21)

Parameters Online Table XXIV

Ribulose-5-phosphate-isomerase (RPI)

R5P → Rb5P

$$v_{RPI} = \frac{Vmax_{21}*(\mathrm{Ru5P}-\frac{R5P}{Keq_{21}})}{Ru5P + Kru5p_{21}*(1+\frac{R5P}{Kr5p_{21}})}$$

(Eq. 22)

Parameters Online Table XXV

Ribulose-5-phosphate-3-epimerase (RPE)

Ru5P → X5P

$$v_{RPI} = \frac{Vmax_{22}*(\mathrm{Ru5P}-\frac{X5P}{Keq_{22}})}{Ru5P + Kru5p_{22}*(1+\frac{X5P}{Kx5p_{22}})}$$

(Eq. 24)

Parameters Online Table XXVI

Transketolase 1 (TK1)

Rb5P + Xu5P <=> G3P + S7P

$$v_{TK1} = k_{23}\mathrm{R5P}*\mathrm{Xu5P} - k_{24}*\mathrm{G3P}*\mathrm{S7P}$$

(Eq. 25)

Parameters Online Table XXVII

Transketolase 2 (TK2)

E4P + Xu5P <=> G3P + F6P

$$v_{TK2} = k_{25}\mathrm{E4P}*\mathrm{Xu5P} - k_{26}*\mathrm{G3P}*\mathrm{F6P}$$

(Eq. 26)

Parameters Online Table XXVIII

Transaldolase (TAL)

G3P + S7P <=> F6P + E4P

$$v_{TAL} = k_{27}\mathrm{G3P}^{*}\mathrm{S7P} - k_{28}{}^{*}\mathrm{E4P}^{*}\mathrm{F6P} \quad \textit{(Eq. 27)}$$

Parameters Online Table XXIX

NADPH oxidase

NADPH → NADP+

$$v_{NADPHoxidase} = k_{29}\mathrm{NADPH} \quad \textit{(Eq. 28)}$$

Parameters Online Table XXX

14. Sample size and power calculation.

Sample size and power calculations for *in vitro*, *in vivo,* and *ex vivo* studies were based on Snedecor et al.[10] and GPower[11] (version 3.1.9.2 for windows). The type 1 error and power were considered at 5% (*P-value* of 0.05) and 80%, respectively. The expected difference in the mean between groups was 50-30%, and the standard deviation 25-12.5%.

15. Statistical Analysis.

Statistical analysis was conducted using R-Studio (version 1.2.1335 for Fedora/RedHat 7 64-bit, R version 3.0.1, Boston, Massachusetts, USA, www.rstudio.com)[12] and GraphPad Prism (version 8.1.2 for Windows, GraphPad Software, La Jolla California USA, www.graphpad.com). Data are represented as mean ± standard error of the mean (s.e.m.) or standard deviation (s.d.). Normal distributed data with two groups were compared using unpaired *t*-test with Welch's correction, and data from three or more groups were compared using one-way analysis of variance (ANOVA) followed by multiple comparison tests (Tukey's method). Non-normal distributed data were analyzed using the Kruskal-Wallis test with Dunn's correction for multiple comparisons.

Unsupervised hierarchical clustering was conducted using R-Studio. The similarity between samples was assessed using a Euclidean distance and the complete agglomeration method. The number of clusters was determined using the k-means algorithm. We applied both the Elbow method and the Bayesian inference criterion to determine optimal numbers of clusters. Heatmaps were generated using R-Studio with the heatmap.2 function from the R-package gplots (version 3.0.1.1). A *P*-value less than 0.05 was considered statistically significant.

ONLINE FIGURES AND FIGURE LEGENDS

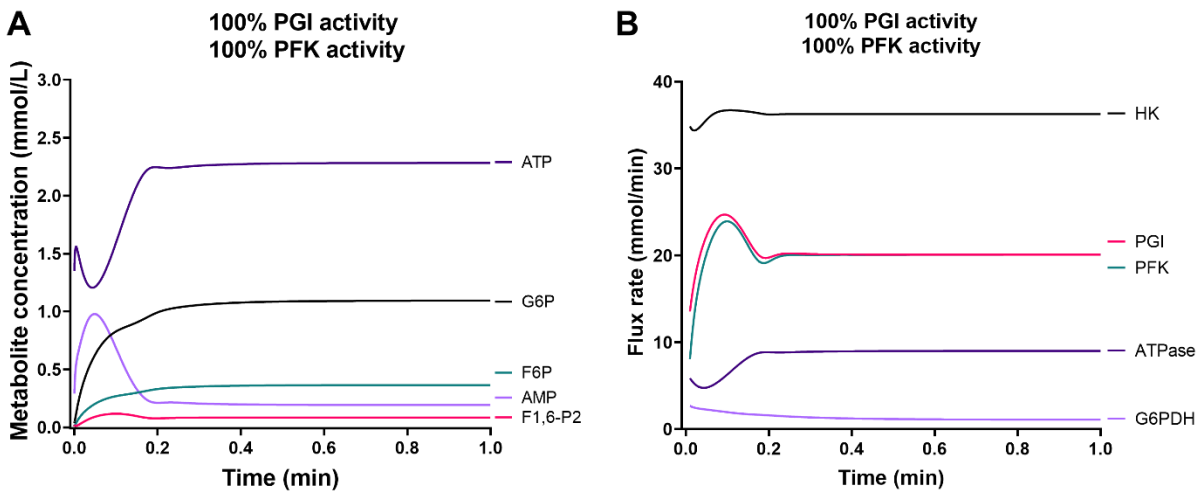

Online Figure I. Time course simulation of CardioGlyco with PPP reactions. (**A**) Predicted metabolite concentrations of ATP, AMP, G6P, F6P, and Fructose 1,6-bisphosphate as a function of time. Extracellular glucose concentration was set to 5.5 mmol/L (**B**) Flux rate changes over time for HK, PGI, PFK, ATPase, and G6PDH with PGI and PFK activity at 100%.

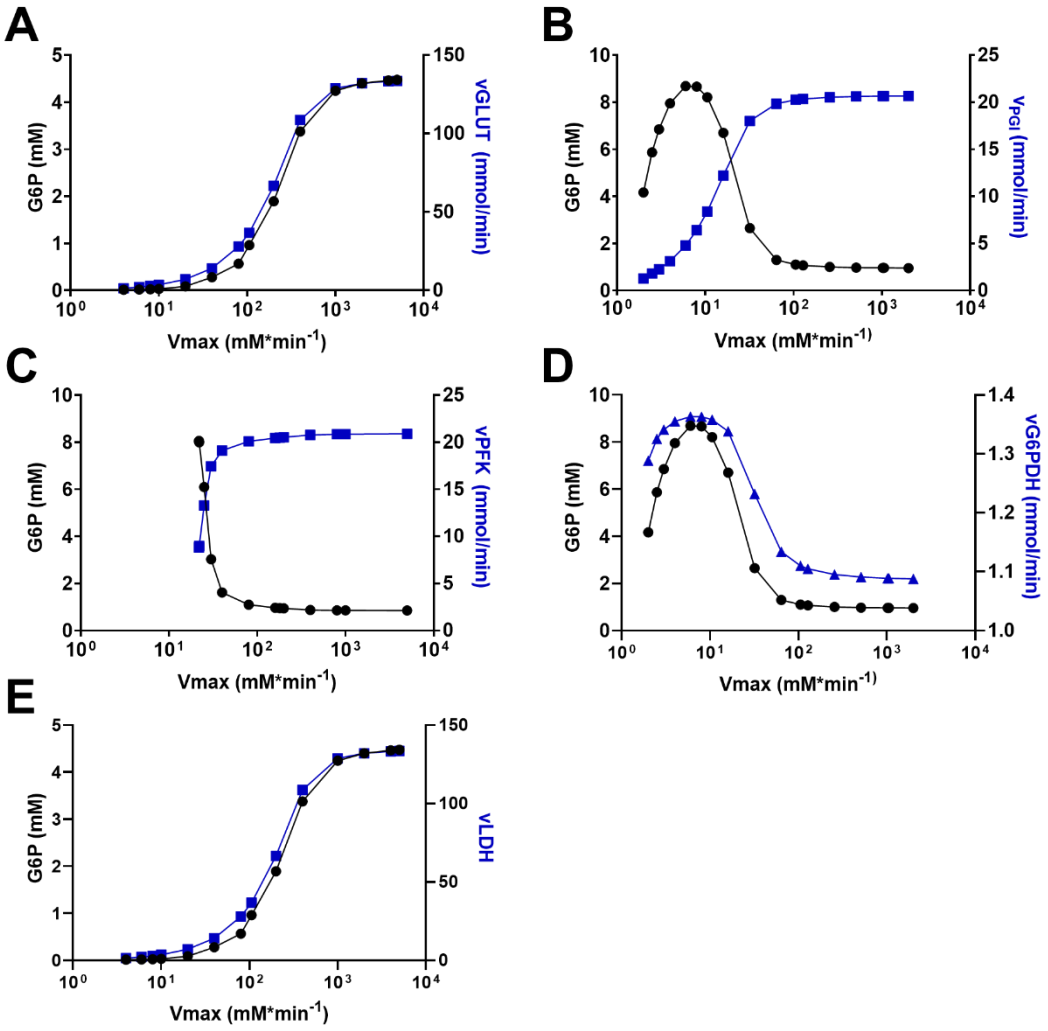

Online Figure II. Relationship between G6P concentration, enzyme activities, and flux rates. Simulations were conducted using the expanded *CardioGlyco* model with PPP reactions. (**A**) G6P concentration and glucose uptake flux (*vGLUT*) as a function of glucose transport (GLUT). (**B**) G6P concentration and PGI flux (*vPGI*) as a function of PGI activity. (**C**) G6P concentration and PFK flux (*vPFK*) as a function of PGI activity. (**D**) G6P concentration and G6PDH flux (*vG6PDH*) as a function of G6PDH activity. (**E**) G6P concentration and LDH flux (*vLDH*) as a function of LDH activity.

ONLINE TABLES AND SUPPORTING INFORMATION

Online Table I. Parameters for *GLUT*.

Parameter	*Value*	*Units*	*Reference*
$Vmax_1$	106	mmol/(min*L)	[8, 13]
$Kglc_1$	10	mmol/L	[8, 13]
Ki_1	0.91		

Online Table II. Parameters for *HK*.

Parameter	*Value*	*Units*	*Reference*
$Vmax_2$	230	mmol/(min*L)	[14, 15]
$Kglc_2$	0.23	mmol/L	[14, 15]
$Kg6p_2$	5.4	mmol/L	[14, 15]
Keq_2	2000		[16]
$Katp_2$	0.78	mmol/L	[14, 15]
$Kadp_2$	0.54	mmol/L	[14, 15]

Online Table III. Parameters for *PGI*.

Parameter	*Value*	*Units*	*Reference*
$Vmax_3$	604	mmol/(min*L)	[8]
$Kg6p_3$	0.425	mmol/L	[8]
$Kf6p_3$	0.3	mmol/L	[16]
Keq_3	0.28		[16, 17]

Online Table IV Parameters for *PFK.*

Parameter	*Value*	*Units*	*Reference*
$Vmax_4$	80	mmol/min	[5, 7]
$Katp_4$	0.71	mmol/L	[5, 7]
$Kamp_4$	0.0995	mmol/L	[5, 7]
$Kf16dp_4$	0.111	mmol/L	[5, 7]
$Kf26p_4$	0.000682	mmol/L	[5, 7]
$Kf6p_4$	1.5	mmol/L	[5, 7]
$Kiatp_4$	0.65	mmol/L	[5, 7]
$Ciatp_4$	100		[5, 7]
$Camp_4$	0.0845		[5, 7]
$Cf26p_4$	0.0174		[5, 7]

$Cf16p_4$	0.397		[5, 7]
$Catp_4$	3		[5, 7]
gR_4	5.12		[5, 7]
$L0_4$	0.66		[5, 7]

Online Table V. Parameters for *ALD.*

Parameter	*Value*	*Units*	*Reference*
$Vmax_5$	94.69	mmol/(min*L)	[8]
$Kig3p_5$	10	mmol/L	[16]
$Kg3p_5$	2.4	mmol/L	[16]
$Kf16bp_5$	0.3	mmol/L	[8]
Keq_5	0.069	mmol/L	[16]
$Kdhap_5$	2	mmol/L	[16]

Online Table VI. Parameters for *TPI.*

Parameter	*Value*	*Units*	*Reference*
$Kdhap_6$	450000	mmol/L	[16]
$Kg3p_6$	1000000	mmol/L	[16]

Online Table VII. Parameters for *PGK.*

Parameter	*Value*	*Units*	*Reference*
$Vmax_7$	1288	mmol/(min*L)	[8]
$Kp3g_7$	0.53	mmol/L	[8]
Keq_7	3200		[16]
$Kbpg_7$	0.003	mmol/L	[8]
$Katp_7$	0.3	mmol/L	[8]
$Kadp_7$	0.2	mmol/L	[8]

Online Table VIII. Parameters for *PGM.*

Parameter	*Value*	*Units*	*Reference*
$Vmax_8$	2585	mmol/(min*L)	[16, 17]
$Kp2g_8$	0.08	mmol/L	[16, 17]
Keq_8	0.19		[16, 17]
$Kp3g_8$	1.2	mmol/L	[16, 17]

Online Table IX. Parameters for *ENO.*

Parameter	*Value*	*Units*	*Reference*
$Vmax_9$	201.6	mmol/(min*L)	[17]
$Kpep_9$	0.5	mmol/L	[17]
$Kp2g_9$	0.04	mmol/L	[17]
Keq_9	2.8	1	[17]

Online Table X. Parameters for *PK.*

Parameter	*Value*	*Units*	*Reference*
$Vmax_{10}$	1000	mmol/(min*L)	[16]
$Kpep_{10}$	0.14	mmol/L	[16]
$Kpyr_{10}$	21	mmol/L	[16]
Keq_{10}	6500		[16]
$Katp_{10}$	1.5	mmol/L	[16]
$Kadp_{10}$	0.53	mmol/L	[16]

Online Table XI. Parameters for *PDC.*

Parameter	*Value*	*Units*	*Reference*
$Vmax_{11}$	857.8	mmol/(min*L)	[8]
$Kpyr_{11}$	4.33	mmol/L	[8]
nH_{11}	1.9		[8]

Online Table XII. Parameters for *AK.*

Parameter	*Value*	*Units*	*Reference*
$Katp_{12}$	45	mmol/L	[16]
$Kadp_{13}$	100	mmol/L	[16]

Online Table XIII. Parameters for *GPDH.*

Parameter	*Value*	*Units*	*Reference*
$Vmax_{14}$	47.11	mmol/(min*L)	[8]
$Knadh_{14}$	0.023	mmol/L	[8]
$Knad_{14}$	0.93	mmol/L	[8]
$Kglycerol_{14}$	1	mmol/L	[8]
$Kdhap_{14}$	0.4	mmol/L	[8]

Keq_{14}	4300		[8]

Online Table XIV. Parameters for *LacT.*

Parameter	*Value*	*Units*	*Reference*
$Vmax_{15}$	400	mmol/(min*L)	[18]
Keq_{15}	1		[18]

Online Table XV. Parameters for *LDH.*

Parameter	*Value*	*Units*	*Reference*
$Vmax_{16}$	2800000	mmol/(min*L)	[19]
Keq_{16}	39000		[19]

Online Table XVI. Parameters for *GAPDH.*

Parameter	*Value*	*Units*	*Reference*
$Vmax_{17}$	22620	mmol/(min*L)	[20]
$Knadh_{17}$	0.06	mmol/L	[20]
$Knad_{17}$	0.09	mmol/L	[20]
$Kg3p_{17}$	0.41	mmol/L	[20]
$Kbpg_{17}$	0.0098	mmol/L	[20]
Keq_{17}	0.000192	FG	[20]

Online Table XVII. Parameters for *GS.*

Parameter	*Value*	*Units*	*Reference*
$Katp_{18}$	6	mmol/L	[17]

Online Table XVIII. Parameters for *ATPase.*

Parameter	*Value*	*Units*		*Reference*
$Katp_{19}$	3.95	mmol/L		[17]

Online Table XIX. Fixed parameters

Parameter	*Value*	*Units*	*Reference*
Glycogen	0.01	mmol/(min*L)	[17]

Online Table XX. Initial metabolite concentrations used for flux predictions.

#	*Name*	*Symbol*	*Initial Value (mmol/L)*	*Reference*
1	Glucose, external	Glc(ext)	5.5	
2	Glucose, cytosolic	Glc(int)	0.1	
3	Glucose 6-phosphate	G6P	0.049	[17]
4	Glycogen	Glycogen	0.01	[17]
5	Fructose 6-phosphate	F6P	0.008	[17]
6	Dihydroxyacetone phosphate	DHAP	0.014	[17]
7	Fructose-1,6-bisphosphate	F1,6-P2	0.02	[21]
8	Glyceraldehyde-3-phosphate	G3P	0.036	[17]
9	1,3-bisphosphoglycerate	BPG	0.00074	[17]
10	2-Phosphoglycerate	P2G	0.001	[17]
11	3-Phosphoglycerate	P3G	0.008	[17]
12	Phosphenolpyruvate	PEP	0.063	[17]
13	Glycerol	Glycerol	0.15	[17]
14	Pyruvate	Pyr	0.003	[17]
15	Lactate	Lac	0.151	[17]
16	Nicotinamide adenine dinucleotide (oxidized)	NAD	1.5	[17]
17	Nicotinamide adenine dinucleotide (reduced)	NADH	0.09	[17]
18	Adenine triphosphate nucleotide	ATP	1.349	[21]
19	Adenine diphosphate nucleotide	ADP	1.28	[21]
20	Adenine monophosphate nucleotide	AMP	0.02	[21]

Online Table XXI. Comparison of model predictions and experimental data.
Metabolite concentrations are often reported in nanomoles per gram dry weight of tissue or micromoles per gram protein. As previously described by Vinnakota K.C. et al. [22], reports on metabolite concentrations in the heart are inconsistent and incomplete. We based our comparison on experimental data mostly from perfused rat hearts. For unit conversions, we used an average tissue density of 1.0526 g/mL and cytosolic water space of 1.9 mL/ g dry weight, 0.399 mL/ g total heart tissue, and 2.27 mL/ g protein.

Metabolite	***Predicted (mmol/L)***	***Observed (mmol/L)***	***References***
Glc(ext)	5.500	5.5	This study
Glc(int)	0.0927		
G6P	0.8393	0.014 ± 0.001 – 1.626 ± 0.508	[8]
F6P	0.2765	0.041 ± 0.009 – 0.321 ± 0.053	[8]
Fru1,6-P2	0.1199	0.016 ± 0.0001 – 0.040 ± 0.002	[8]
DHAP	0.0313	0.017 ± 0.004 – 0.158 ± 0.056	[8, 23]
G3P	0.0014	0.0319 – 2.5 ± 0.042	[7, 8]
BPG	0.0002	0.0007	[24]
P3G	0.1367	0.071 ± 0.004 – 0.4512	[7, 8]
P2G	0.0208	0.009 ± 0.002 – 0.0526	[7, 8]
PEP	0.0212	0.01 – 0.13 ± 0.003	[7, 8]
Pyr	0.0063	0.036 ± 0.003 – 0.085 ± 0.004	[7, 8]
Lac	0.1066	0.288 ± 0.064 – 0.87 ± 0.01	[7, 8]
ATP	3.0417	3.45 ± 0.09	[23]
ADP	0.7700	0.685 ± 0.014	[23]
AMP	0.4332	0.110 ± 0.016	[23]
NAD	3.2962	3.00 ± 0.09	[24]
NADH	0.0038	0.276 ± 0.2	[24]

Online Table XXII. Parameters for *G6PDH.*

Parameter	*Value*	*Units*	*Reference*
$Vmax_{18}$	1134	mmol/(min*L)	[25]
$Knadph_{18}$	0.017	mmol/L	[26]
$Knadp_{18}$	0.045	mmol/L	[26]
$Kg6p_{18}$	0.042	mmol/L	[26]
$K6pgl_{18}$	0.1	mmol/L	[26]

Online Table XXIII. Parameters for *GL.*

Parameter	*Value*	*Units*	*Reference*
$Vmax_{19}$	17.76	mmol/(min*L)	[26]
$K6pg_{19}$	0.1	mmol/L	[26]
$K6pgl_{19}$	0.8	mmol/L	[26]

Online Table XXIV. Parameters for *6PGDH.*

Parameter	*Value*	*Units*	*Reference*
$Vmax_{20}$	562.8	mmol/(min*L)	[26]
$K6pg_{20}$	0.115	mmol/L	[26]
$Kr5p_{20}$	0.1	mmol/L	[26]
$Knadp_{20}$	0.094	mmol/L	[26]
$Knadph_{20}$	0.055	mmol/L	[26]

Online Table XXV. Parameters for *RPI.*

Parameter	*Value*	*Units*	*Reference*
$Vmax_{21}$	1005	mmol/(min*L)	[26]
$Kru5p_{21}$	2.47	mmol/L	[26]
$Kr5p_{21}$	5.7	mmol/L	[26]
Keq_{21}	4	mmol/L	[26]

Online Table XXVI. Parameters for *RPE.*

Parameter	*Value*	*Units*	*Reference*
$Vmax_{22}$	7236	mmol/(min*L)	[26]
$Kru5p_{22}$	5.97	mmol/L	[26]
$Kx5p_{22}$	7.7	mmol/L	[26]

Keq_{22}	1.4	mmol/L	[26]

Online Table XXVII. Parameters for TK1.

Parameter	*Value*	*Units*	*Reference*
K_{23}	0.006	L/(mmol*min)	[26]
K_{24}	0.1	L/(mmol*min)	[26]

Online Table XXVIII. Parameters for TK2.

Parameter	*Value*	*Units*	*Reference*
K_{25}	0.75	L/(mmol*min)	[27]
K_{26}	0.1	L/(mmol*min)	[27]

Online Table XXIX. Parameters for TAL.

Parameter	*Value*	*Units*	*Reference*
K_{27}	1.65	L/(mmol*min)	[26]
K_{28}	0.1	L/(mmol*min)	[26]

Online Table XXX. Parameters for *NADPH oxidase.*

Parameter	*Value*	*Units*	*Reference*
K_{29}	100	1/min	[26]

Online Table XXXI. Initial metabolite concentrations used for pentose phosphate pathway intermediates.

#	***Name***	***Symbol***	***Initial Value (mmol/L)***	***Reference***
21	Nicotinamide adenione dinucleotide phosphate (reduced)	NADPH	0.015	[28]
22	Nicotinamide adenione dinucleotide phosphate (oxidized)	NADP+	0.009	[27]
23	6-phosphogluconolactone	6PGL	0.008	[27]
24	6-phosphogluconate	6PG	0.008	[27]
25	Ribose-5-phosphate	R5P	0.005	[29]
26	Sedoheptulose-5-phosphate	S5P	0.001	[29]
27	Ribulose-5-phosphate	Ru5P	0.001	[29]
28	Erythrose-4-phosphate	E4P	0.005	[27]
29	Xylulose-5-phosphate	X5P	0.001	[29]

REFERENCES

1. Goodwin GW, Ahmad F, Doenst T, Taegtmeyer H. Energy provision from glycogen, glucose, and fatty acids on adrenergic stimulation of isolated working rat hearts. *Am J Physiol*. 1998;274:H1239-H1247
2. Ma Y, McClatchy DB, Barkallah S, Wood WW, Yates JR, 3rd. Quantitative analysis of newly synthesized proteins. *Nat Protoc*. 2018;13:1744-1762
3. Hoops S, Sahle S, Gauges R, Lee C, Pahle J, Simus N, Singhal M, Xu L, Mendes P, Kummer U. Copasi--a complex pathway simulator. *Bioinformatics*. 2006;22:3067-3074
4. Karlstädt A, Fliegner D, Kararigas G, Ruderisch HS, Regitz-Zagrosek V, Holzhütter H-G. Cardionet: A human metabolic network suited for the study of cardiomyocyte metabolism. *BMC Syst Biol*. 2012;6:114
5. Hulme EC, Tipton KF. The isotope-exchange reactions of ox heart phosphofructokinase. *Biochem J*. 1971;122:181-187
6. Hulme EC. Simulation of biochemical systems. *J Theor Biol*. 1971;31:131-137
7. Pogson CI, Randle PJ. The control of rat-heart phosphofructokinase by citrate and other regulators. *Biochem J*. 1966;100:683-693
8. Kashiwaya Y, Sato K, Tsuchiya N, Thomas S, Fell DA, Veech RL, Passonneau JV. Control of glucose utilization in working perfused rat heart. *J Biol Chem*. 1994;269:25502-25514
9. Wu F, Zhang EY, Zhang J, Bache RJ, Beard DA. Phosphate metabolite concentrations and atp hydrolysis potential in normal and ischaemic hearts. *J Physiol*. 2008;586:4193-4208
10. Snedecor GW CW. *Statistical methods*. Iowa State University Press; 1989.
11. Faul F, Erdfelder, E., Lang, A.-G., Buchner, A. G*power 3: A flexible statistical power analysis program for the social, behavioral, and biomedical sciences. *Behavior Research Methods*. 2007;3:175-191
12. Loraine AE, Blakley IC, Jagadeesan S, Harper J, Miller G, Firon N. Analysis and visualization of rna-seq expression data using rstudio, bioconductor, and integrated genome browser. *Methods Mol Biol*. 2015;1284:481-501
13. Cheung JY, Conover C, Regen DM, Whitfield CF, Morgan HE. Effect of insulin on kinetics of sugar transport in heart muscle. *Am J Physiol*. 1978;234:E70-78
14. Grossbard L, Schimke RT. Multiple hexokinases of rat tissues. Purification and comparison of soluble forms. *J Biol Chem*. 1966;241:3546-3560
15. Doenst T, Han Q, Goodwin GW, Guthrie PH, Taegtmeyer H. Insulin does not change the intracellular distribution of hexokinase in rat heart. *Am J Physiol*. 1998;275:E558-567
16. Williamson JR. Glycolytic control mechanisms. I. Inhibition of glycolysis by acetate and pyruvate in the isolated, perfused rat heart. *J Biol Chem*. 1965;240:2308-2321

17. Donohoe JA, Rosenfeldt FL, Munsch CM, Williams JF. The effect of orotic acid treatment on the energy and carbohydrate metabolism of the hypertrophying rat heart. *Int J Biochem*. 1993;25:163-182
18. Evans RK, Scoville CR, Ito MA, Mello RP. Upper body fatiguing exercise and shooting performance. *Mil Med*. 2003;168:451-456
19. Borgmann U, Moon TW, Laidler KJ. Molecular kinetics of beef heart lactate dehydrogenase. *Biochemistry*. 1974;13:5152-5158
20. Knight RJ, Kofoed KF, Schelbert HR, Buxton DB. Inhibition of glyceraldehyde-3-phosphate dehydrogenase in post-ischaemic myocardium. *Cardiovasc Res*. 1996;32:1016-1023
21. Nascimben L, Ingwall JS, Lorell BH, Pinz I, Schultz V, Tornheim K, Tian R. Mechanisms for increased glycolysis in the hypertrophied rat heart. *Hypertension*. 2004;44:662-667
22. Vinnakota KC, Bassingthwaighte JB. Myocardial density and composition: A basis for calculating intracellular metabolite concentrations. *Am J Physiol Heart Circ Physiol*. 2004;286:H1742-1749
23. Narabayashi H, Lawson JW, Uyeda K. Regulation of phosphofructokinase in perfused rat heart. Requirement for fructose 2,6-bisphosphate and a covalent modification. *J Biol Chem*. 1985;260:9750-9758
24. Kobayashi K, Neely JR. Control of maximum rates of glycolysis in rat cardiac muscle. *Circ Res*. 1979;44:166-175
25. Ata H, Rawat DK, Lincoln T, Gupte SA. Mechanism of glucose-6-phosphate dehydrogenase-mediated regulation of coronary artery contractility. *Am J Physiol Heart Circ Physiol*. 2011;300:H2054-2063
26. Ghaemmaghami S, Huh WK, Bower K, Howson RW, Belle A, Dephoure N, O'Shea EK, Weissman JS. Global analysis of protein expression in yeast. *Nature*. 2003;425:737-741
27. Gumaa KA, McLean P. The pentose phosphate pathway of glucose metabolism. Enzyme profiles and transient and steady-state content of intermediates of alternative pathways of glucose metabolism in krebs ascites cells. *Biochem J*. 1969;115:1009-1029
28. Gupte SA, Levine RJ, Gupte RS, Young ME, Lionetti V, Labinskyy V, Floyd BC, Ojaimi C, Bellomo M, Wolin MS, Recchia FA. Glucose-6-phosphate dehydrogenase-derived nadph fuels superoxide production in the failing heart. *J Mol Cell Cardiol*. 2006;41:340-349
29. Zuurbier CJ, Eerbeek O, Goedhart PT, Struys EA, Verhoeven NM, Jakobs C, Ince C. Inhibition of the pentose phosphate pathway decreases ischemia-reperfusion-induced creatine kinase release in the heart. *Cardiovasc Res*. 2004;62:145-153